



## Research Article

# Comparison of speed control techniques in field oriented control of permanent magnet synchronous motor: Lyapunov approach

Ahmet İlkkan AÇIKGÖZ<sup>1,\*</sup>, İbrahim ALIŞKAN<sup>2</sup>

<sup>1</sup>Department of Electronics and Automation, Zonguldak Vocational School, Zonguldak Bülent Ecevit University, Zonguldak, 67500, Türkiye

<sup>2</sup>Department of Control and Automation Engineering, Faculty of Electrical & Electronics, Yıldız Technical University, İstanbul, 34349, Türkiye

## ARTICLE INFO

### Article history

Received: 13 November 2021

Revised: 25 December 2021

Accepted: 05 April 2022

### Keywords:

PMSM; Speed Control, Signal Smoothing; Nonlinear Control; FOC; Vector Control; SVPWM; Lyapunov Function; PI; Barbalat's Lemma; Stability Analysis; RMSE; ITAE

## ABSTRACT

The main focus of this study is the minimization of Permanent Magnet Synchronous Motors (PMSM) steady-state speed error. In order to do this, a Lyapunov candidate function that contained the speed error is defined and a Based Lyapunov Theory (BLT) speed controller is designed. The novelty of this paper is the smoother pre-filter applied to the reference speed guarantees the stable operation of the nonlinear controller at step change in reference signal. The pre-filter design is carried out in a way that does not have a negative effect on the settling time, which is one of the step response characteristics. A proportional-integral (PI) speed controller is designed for comparison. FOC technique is used for inverter control. As the speed controller of the system, PI and BLT controllers are designed separately. Simulation studies are run in MATLAB/Simulink. PI speed controller coefficients are determined using the pole assignment method. For this purpose, PI coefficients for operating the controller at the selected frequency and the desired damping ratio are calculated. Stability analyses are carried out for PI and BLT speed controllers. A low pass filter that allows the system to apply a smoothed reference speed is designed in order to eliminate the range in which the derivative of the reference speed used in the BLT speed controller is undefined. Three different simulations are modeled. In the first one, the reference speed is changed in both directions by step function, under constant load torque. The speed and torque performances of both speed controllers are compared with the performance criteria including settling time, overshoot, peak value, peak time, root mean squared error (RMSE), and integral of time weighed absolute error (ITAE), and the results of the comparison are shown in figures and tables. In addition, a second simulation including reference load changes is made to model load torque disturbance as a robustness test, and a third simulation containing resistance changes is made to model parameter uncertainty are carried out. Both transient response and steady state response of controllers against parameter changes are examined in simulation 2 and 3. With the proposed BLT controller, the transient and steady-state response of the speed is improved both at the time of torque change and at the time of winding resistance change. The results are given in figures and tables.

**Cite this article as:** Açıkgöz Aİ, Alışkan İ. Comparison of speed control techniques in field oriented control of permanent magnet synchronous motor: Lyapunov approach. Sigma J Eng Nat Sci 2023;41(6):1177–1196.

### \*Corresponding author.

\*E-mail address: [ilkkanacikgoz@gmail.com](mailto:ilkkanacikgoz@gmail.com)

This paper was recommended for publication in revised form by Regional Editor Ahmet Selim Dalkılıç



## INTRODUCTION

Since the development of magnetic materials such as samarium-cobalt in the 1970s and neodymium-iron-boron (NdFeB) in the 1980s which provide cheaper and higher magnetic flux density enabled the increase of the power range of PMSMs from kW to MW which allowed PMSMs to replace DC motors in many high-performance applications [1]. PMSM shine out in medium-low power applications with their high power density, robust construction and small size, low maintenance cost, high efficiency, reliability, low noise and inertia, and good dynamic performances like high torque/current and torque/inertia ratios. Therefore, their use in high-performance applications such as industrial servo systems is becoming increasingly popular among researchers and designers [2-7].

Various types of electric motors are available for drive applications such as electric vehicles and robot manipulators. PMSMs draw special attention in electric vehicle drive applications due to their higher power to size density, higher efficiency and less maintenance requirements than other existing motors [9]. Unlike conventional synchronous motors, PMSMs do not have excitation winding which eliminates rotor copper losses [11,12]. The most important configurations of PMSMs are surface mounted PMSM (SPMSM) and interior mounted permanent magnet (IPMSM). Although the magnets are mounted on the rotor surface, the effective air gap is homogeneous and wide, since the relative permeability of the magnetic material is close to unity. Therefore, the synchronous inductances along the d and q axes of the rotor are equal and small [2]. Because of its aforementioned superior properties, studies on PMSM are continuing [7, 13-16].

Adjustable speed alternating current (AC) motor drives with electronic power converters make more use of FOC and direct torque control (DTC) techniques in various applications [17-20]. In practice, main PMSM torque control methods are FOC and DTC [7, 9, 14-16]. FOC has better performance than DTC in wider speed range and load conditions. The performance of FOC application is critically dependent on very precise coordinated transformations and flux angle estimations. This complexity leads to considerably more calculations [18]. Additionally, the FOC method is more easily applied in these motors than in other motors, because of the constant magnetic flux generated by the permanent magnets placed in the rotor of the PMSMs [2]. This technique is preferred in order to reduce the complexity of PMSMs with this approach [16]. This technique allows the PMSM to be driven with higher dynamic performance which is comparable to the performance of the DC motor [2]. If the d current component  $i_d$  can be made equal to zero, the exact behavior of a constant excited DC motor can be achieved [23]. In this technique, the dynamic model of the motor is used in the design of the controller, instead of the steady-state model on which the scalar controllers are based [2]. FOC is a vector control technique

that provides high precision as well as high motor control speed. However, the main criticism of the FOC is related to the imbalance problem, which may be caused by possible changes in the motor parameters of the system or disturbances during operation and numerous calculations limiting the control speed [24].

Different pulse width modulation (PWM) techniques can be used in FOC [24,25]. Space vector pulse width modulation (SVPWM) used in this study is one of the voltage controlled, constant switching frequency PWM switching strategies [2]. It is known that SVPWM performs better than sinusoidal pulse width modulation (SPWM) [25]. SVPWM technique is widely used in PMSM [7,14, 15].

It is important to improve PMSM control performance for many PMSM applications [26]. PI controller is a conventional control method which is frequently used in control systems [14,27]. Moreover, it also commonly used in controlling PMSM with FOC method. [7,13,16,28]. The PI controller is mainly used to eliminate the steady-state error caused by the proportional (P) controller. However, it has a negative impact on the speed of response and the overall stability of the system. The PI controller is mostly applicable to systems where the response speed of the system is not a problem. Since the PI controller is not capable of predicting future errors of the system, it cannot reduce the rise time and eliminate oscillations. The integral calculations used in the controller ensures the set point being exceeded [29].

Some of PI tuning techniques are as follows; open and closed-loop Ziegler-Nichols (ZN) method [27, 29, 31], frequency response/domain method [28,32,33,34], and pole assignment/placement method [35-40]. Open loop ZN method cannot be applied to systems which are type one and above. In case it is attempted to be implemented, the open loop response will result in infinity due to the integrator in which  $\lim_{t \rightarrow \infty} y(t) \rightarrow \infty$  status is encountered where the output of the system is  $y(t)$ . On the other hand, in practical applications the system becomes saturated. Frequency response/domain methods focus on the frequency domain characteristics of the control system [33]. In this method, design tools such as root locus, bode plots, nyquist diagrams and nichols chart are used [8]. By applying frequency domain design methods, control parameters that are based on different specification types that define design requirements for system stability and robustness, such as gain crossover frequency, phase margin, phase crossover frequency, gain margin, and sensitivity functions can be analytically calculated [33]. Pole assignment/placement technique is applied for tuning PI controller of PMSM. The main idea behind the polar placement approach is selecting the appropriate closed-loop performance which takes desired  $\xi$  and desired  $w_n$  as its basis. The denominator of the closed-loop transfer function is equalized to the desired closed-loop polynomial. In order to apply the polar placement technique, a first or second order model of the plant is required [39]. Second order system approach can be used in speed controller design for PMSM [26]. Thus, PI speed controller

which can provide the desired speed response with appropriate  $\xi$ ,  $w_n$  values is designed [40].

Stability analyses of differential equations using energy functions has been performed by Lyapunov in 1892 [41] and ever since Lyapunov theory has been an important tool in linear and nonlinear control [42-46]. Nevertheless, its use in nonlinear control has difficulties in finding the Lyapunov function for a given system. The system is known to be stable if Lyapunov function appropriate for the system can be found. But the task of finding such a function is usually left to the designer's experience [42]. The BLT control technique is a mathematical acquisition of a control signal giving the alteration that enable the function to exponentially approaching to zero by determining an energy function connected to the error signal [47]. It is also known that control systems based on Lyapunov function give more effective results in the control of nonlinear systems [42,48].

In addition to the simulation results that compares both of the designed speed controller against the reference speed changes, a second simulation is carried out which includes reference load changes in order to model load torque disturbance as well as performing the robustness test and a third simulation study that includes resistance changes to model parameter uncertainty performed and all the performances are compared.

The aim of this study is to design an effective and simple speed control for PMSM with Lyapunov approach. In the system designed in this study, fast transient response, a good steady-state response, acceptable accuracy are aimed. In the presence of external loads and load disturbances, the system output with the Lyapunov function is achieved this purpose step-by-step. Lyapunov function which included a term that enhances stability and penalizes the incremental energy of the speed error is used in the proposed speed control system. The proposed control system is designed to achieve the speed tracking target.

In this study, BLT speed controller is developed for PMSMs. The main problem encountered in speed controllers developed based on Lyapunov theory is that if step function speed is used as reference speed, high amplitude control signals seen in speed changes caused by the derivative of the reference signal used in the controller function. In order to solve this problem, a low-pass filter appropriate for system dynamics is applied to the reference signal and the derivative effect that causes high amplitude is eliminated. The compatibility between the developed filter and the proposed BLT speed controller has been confirmed by simulation studies. The performance values of the PI controller designed with the pole assignment method have also been another scale confirming the success of the proposed control structure.

The paper is organized as follows. The mathematical model of PMSM is described in Chapter 2. The SVPWM method is explained in Chapter 3. FOC, PI and BLT controllers, PI and Lyapunov stability analyses, and the deactivation of the range in which the derivative is undefined are

given in Chapter 4. Chapter 5 presents information about the simulations. The results and discussion are given in Chapter 6. The conclusion is informed in Chapter 7.

### Mathematical Model of PMSM

The mathematical model of PMSM can be expressed using three different equations for three state variables in the d-q framework as follows: [8,23,24,40]:

$$V_d = Ri_d + p\lambda_d - w\lambda_q \quad (1)$$

$$V_q = Ri_q + p\lambda_q + w\lambda_d \quad (2)$$

Here,

$$\lambda_q = L_q i_q \quad (3)$$

$$\lambda_d = L_d i_d + \lambda_m \quad (4)$$

Electrical Torque,

$$T_e = \frac{3P}{2} [\lambda_m i_q + (L_d - L_q) i_d i_q] \quad (5)$$

Motor dynamic equation,

$$T_e = T_L + Bw_r + J \frac{dw_r}{dt} \quad (6)$$

The inverter frequency is related to the motor speed and is as follows;

$$w = Pw_r \quad (7)$$

As a result, the dynamic model of PMSM (nonlinear state equations) is as follows;

$$\frac{di_d}{dt} = -\frac{R}{L_d} i_d + \frac{Pw_r L_q}{L_d} i_q + \frac{1}{L_d} V_d \quad (8)$$

$$\frac{di_q}{dt} = -\frac{R}{L_d} i_q + \frac{Pw_r L_d}{L_q} i_d - \frac{P\lambda_m}{L_q} w_r + \frac{1}{L_q} V_q \quad (9)$$

$$\frac{dw_r}{dt} = \frac{3P\lambda_m}{2J} i_q + \frac{3P}{2J} (L_d - L_q) i_d i_q - \frac{B}{J} w_r - \frac{T_L}{J} \quad (10)$$

It can be seen from this dynamic model that speed control can be controlled via  $V_q$ . For this reason, reference value of  $i_d$  is kept zero. In addition, as stated in the introduction of SPMSM, when  $L_d = L_q = L$  is considered, the SPMSM dynamic model (nonlinear state equations) is formed as follows;

$$\frac{dw_r}{dt} = \frac{3P\lambda_m}{2J} i_q - \frac{B}{J} w_r - \frac{T_L}{J} \quad (11)$$

$$\frac{di_q}{dt} = -\frac{R}{L}i_q + P\omega_r i_d + \frac{P\lambda_m}{L}\omega_r + \frac{1}{L}V_q \quad (12)$$

$$\frac{di_d}{dt} = -\frac{R}{L}i_d + P\omega_r i_q + \frac{1}{L}V_d \quad (13)$$

$$T_e = \frac{3P}{2}(\lambda_m i_q) \quad (14)$$

**SVPWM Method**

SVPWM method is used in the study. Figure 1 shows three-phase two-level voltage source inverter where PWM methods are applied.  $V_a, V_b, V_c$  are applied to star connected PMSM three phase windings.  $V_{dc}$  is continuously applied to the inverter. Three of the inverter switches must be short-circuited and three of them must be open-circuit, at all times. The upper and lower switches on each lever must be driven by two complementary pulse signals, to prevent vertical transmission. In addition, it is important to prevent any possible overlap during the transition between the power switch [25, 49].

A total of 6 power switches (2 for each phase) are used in the inverter given in Figure 1. For each of the levers K1, K2,

and K3, the situation of the above switch being short-circuit and the below switch is open-circuit corresponds to 1, and the opposite situation is expressed with 0. This allows us to examine the 6 power switches using 8 states [25, 49]. The relationship between the switching vectors and the phase voltages is discussed in [50]. Table 1 shows values of the voltage vectors, switching vectors, the inverter phase and line voltages in  $V_{dc}$  unit for the 8 states in the SVPWM [50-52]. Using  $V_a, V_b, V_c$  and Clarke conversion, Equation (15) can be achieved for  $v_\alpha, v_\beta$ .

$$\vec{V} = v_\alpha + jv_\beta = \frac{2}{3} \left( V_a e^{j0} + V_b e^{j\frac{2\omega}{3}} + V_c e^{j\frac{4\omega}{3}} \right) \quad (15)$$

The eight possible states of the inverter are represented by the six active state vectors which constitutes a hexagon and two zero vectors, as shown in Figure 2 [49].

Figure 2 shows the vectors for the remaining cases which can be achieved using the same approach. Six non-zero states, called active states, are represented by space vectors in the form of a hexagon divided into six equal sectors shown in Figure 2 as I, II, III, IV, V, VI. The space vector equation for active states is expressed in Equation (16).

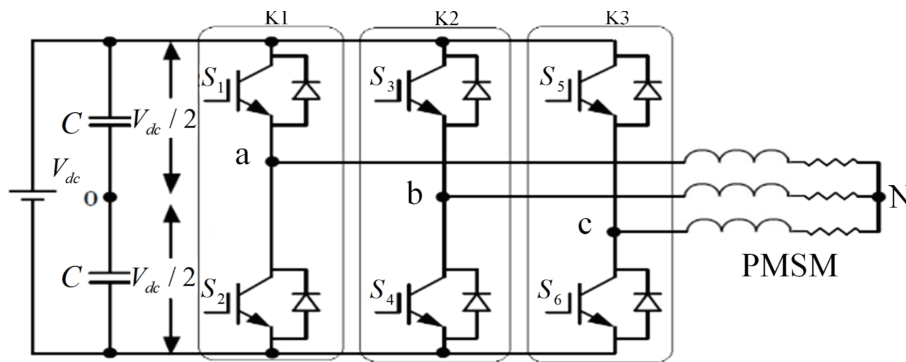


**Figure 1.** Three phase two level voltage source inverter.

**Table 1.** SVPWM voltage and switching vectors, phase and line voltages

Voltage Vectors	Switching Vectors			Phase Voltages			Line Voltages		
	K1	K2	K3	$V_a$	$V_b$	$V_c$	$V_{ab}$	$V_{bc}$	$V_{ca}$
$V_0$	0	0	0	0	0	0	0	0	0
$V_1$	1	0	0	2/3	-1/3	-1/3	1	0	-1
$V_2$	1	1	0	1/3	1/3	-2/3	0	1	-1
$V_3$	0	1	0	-1/3	2/3	-1/3	-1	1	0
$V_4$	0	1	1	-2/3	1/3	1/3	-1	0	1
$V_5$	0	0	1	-1/3	-1/3	2/3	0	-1	1
$V_6$	1	0	1	1/3	-2/3	1/3	1	-1	0
$V_7$	1	1	1	0	0	0	0	0	0

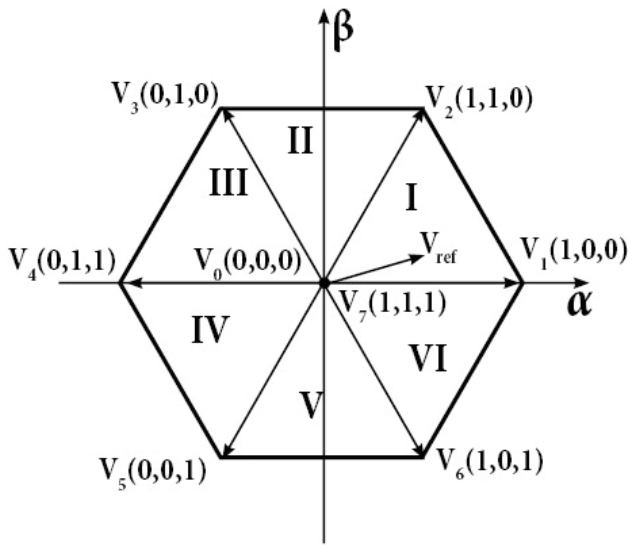


Figure 2. Inverter conditions on static reference framework [49].

$$\vec{V}_k = \frac{2}{3} V_{dc} e^{j(k-1)\frac{\pi}{3}}, k = 1, \dots, 6 \tag{16}$$

$\vec{V}_{ref}$  assuming that  $T_s$  is small enough,  $\vec{V}_{ref}$  can be considered constant, throughout this range. The SVPWM technique is based on the fact that each  $\vec{V}_{ref}$  vector within the hexagonal boundary is expressed as a combination of weighted average of two neighboring active space vectors and the zero state vectors. Thus, the desired reference vector in each cycle can be obtained by switching between these four inverter states. The  $\vec{V}_{ref}$  vector in sector  $k$  is obtained as shown in Equations (17) and (18).

$$\vec{V}_{ref} \frac{T_s}{2} = \vec{V}_k T_k + \vec{V}_{k+1} T_{k+1} \tag{17}$$

$$T_0 + T_k + T_{k+1} = \frac{T_s}{2} \tag{18}$$

## CONTROLLER DESIGNS

### Field Oriented Control

Figure 3 shows the block diagram of the FOC method of PMSM. The measured two phase current of the motor feeds the Clarke conversion block. The two components of the current in this system are converted to the d-q rotating reference framework with Park conversion. Resulting values of  $i_d$  and  $i_q$  are compared to flux reference  $i_{dref}$  and torque reference  $i_{qref}$  respectively. Since FOC is used in speed control, the torque reference  $i_{qref}$  becomes the output of the speed controller. Outputs  $v_{qref}$  and  $v_{dref}$  of classic PI current controller are applied to reverse Park conversion block. The inputs of SVPWM block are  $v_{\alpha ref}$  and  $v_{\beta ref}$  while the outputs are the signals driving the inverter [53,54].

### PI Speed Controller

Pole assignment method which incorporates the closed loop TF of the system is used for this study. For stability, a  $w_c$  must be determined which ensures the root vectors of the characteristic equation of the system are located in the left half of the complex plane as well as the angle of the vectors being between  $30^\circ$  and  $60^\circ$  [28,32,55].  $w_c$  is the frequency in which the low and high frequency asymptotes are equal [55]. In this technique, the trial-and-error method is generally used to dedicate  $w_c$  value [28, 55]. The selected frequency value in this study is 914 rad/s for the second

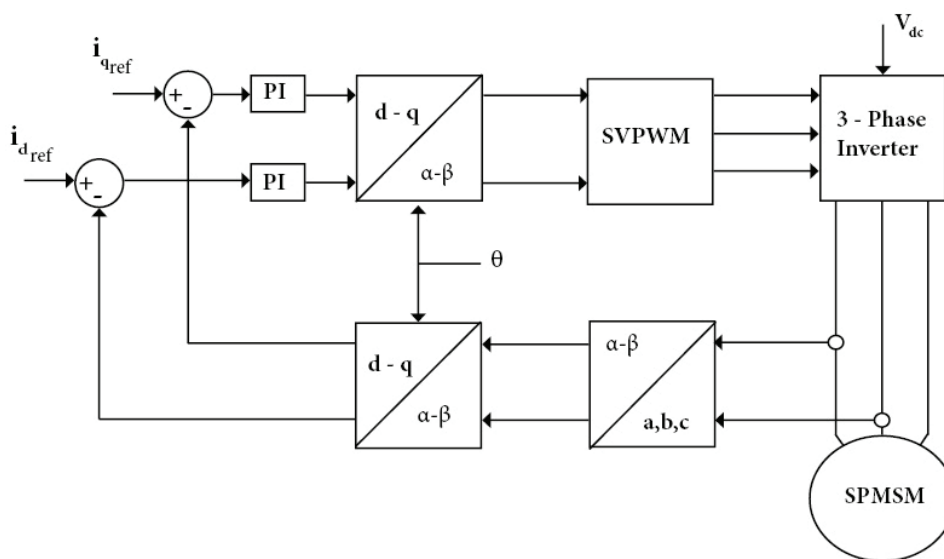


Figure 3. Block diagram for FOC method of PMSM [53].

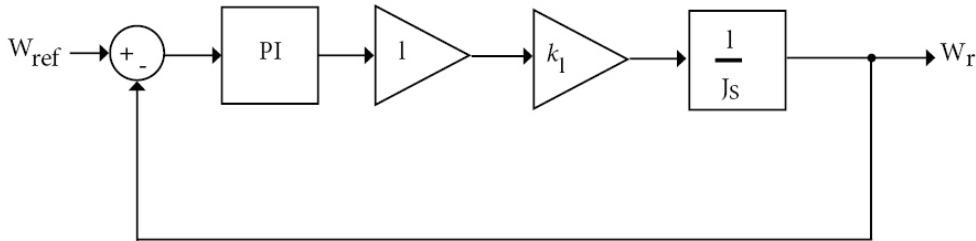


Figure 4. PMSM simple speed loop block diagram [28].

order delayed system. This selected frequency value is used to determine the coefficients  $k_p, k_i$  from the characteristic equation obtained from the simple closed-cycle speed loop of PMSM [28].

The current loop gain in the model given in Figure 4 is chosen as 1 for simplicity. The characteristic equation obtained from the closed-cycle transfer function is a characteristic equation of the second order control system [40]. The TF obtained from this model is shown in Equation (19).

$$TF_{Speed\_loop} = \frac{k_p k_t s + k_i k_t}{J s^2 + k_p k_t s + k_i k_t} \tag{19}$$

The characteristic equation is a second order delay system as follows:

$$s^2 + 2\xi w_0 s + w_0^2 = 0 \tag{20}$$

In a second order delay system, in order for the frequency response to be a sub-critical damped system, the condition is  $\xi < 1$  [55]. For the selected frequency and  $\xi = 0.8$  value of the system, the calculated coefficients of the PI speed controller are as:  $k_i = 64.6875, k_p = 0.1131$

Thus, the coefficients of the PI controller are determined by the pole assignment method for the selected frequency and the damping factor determined to keep the system stable.

**PI Speed Controller Stability Analysis**

For stability, the roots of the characteristic equation of the system must be in the left half of the complex plane [55]. For the calculated PI controller coefficients, the conjugate roots of the characteristic equation are found as:  $S_{1,2} = -731.62 \pm i549.21$

Thus, for the pole assignment method that is used, the roots of the closed-cycle characteristic equation of the system are located in the left half of the complex plane and their angles are between  $30^\circ$  and  $60^\circ$ .

In the rest of the study, the term PI controller is used instead of the term PI speed controller designed with the pole assignment method.

**Lyapunov Theory Based Speed Controller**

If we accept  $x$  as the equilibrium point of the system and make it equal to zero ( $x = 0$ ), stability of equilibrium point can be proven by examining interwoven surfaces described with  $V(x) = C, (C > 0)$  and the positive defined function  $V = V(x)$  surrounding the equilibrium point  $x = 0$ . If  $\dot{V}$  is always negative except at  $x = 0$ , where  $V = 0$ , then  $\dot{V}$  follows the trajectory in which it must pass the  $V$  fixed surface in the inward direction. As a result, point  $x$  tends to be zero while time  $t$  tends to be infinite. The three-dimensional example is shown in Figure 5 which proves the asymptotic stability of the system without requiring an open solution for the system [56].

If the equilibrium point at the origin is uniformly asymptotically stable, there is a positive definite and decreasing function  $V$  with a negative definite derivative [57].

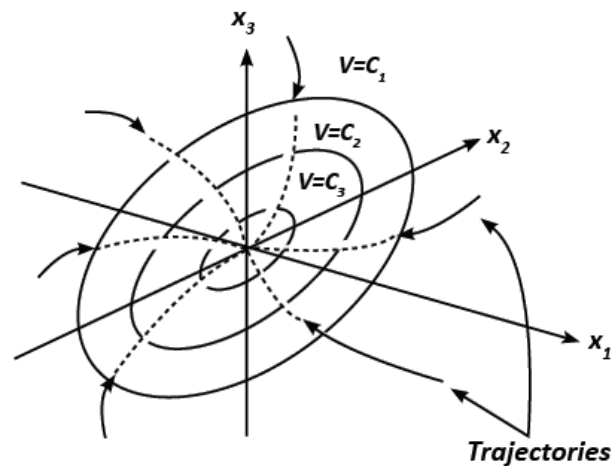


Figure 5. Lyapunov function contours and trajectories [56].

The proposed control system is designed to achieve the reference speed tracking purpose. This objective is used for a systematic approach to construct the Lyapunov equation and unperturbed controller, so that the system is uniformly asymptotically stable at the equilibrium point. [43,44,56]. The speed error signal is defined as follows,

$$e = w_{ref} - w_r \tag{21}$$

If the derivative of Equation (21) is calculated and written instead of Equation (10), Equation (22) is obtained.

$$\dot{e} = \dot{w}_{ref} - \frac{1}{j} \left[ \frac{3P}{2} \left( (L_d - L_q) i_d i_q + \lambda_m i_q \right) - B w_r - T_L \right] \tag{22}$$

In the proposed control system, Barbalat’s Lemma is used to control the robustness against parameter uncertainty, in other words: to perform stability analysis [57]. In the literature, the stability analysis of the BLT speed controller has been performed with Barbalat’s Lemma [58-60], which is used in asymptotic stability analysis of the systems.

Barbalat’s Lemma indicates that if the differentiable function  $v(t)$  has a finite limit as  $t \rightarrow \infty$  and if  $\dot{V}$  is uniformly continuous then  $\dot{V} \rightarrow 0$  as  $t \rightarrow \infty$  [57].

In order to decide the stabilizing function to allow the tracking error to converge to zero, the following positively defined scalar Lyapunov function is determined.

$$V = \frac{1}{2} e^2 \rightarrow v(t) \in R, \begin{cases} V = 0, e = 0 \\ V > 0, e \neq 0 \end{cases} \tag{23}$$

If taken the derivative,

$$\begin{aligned} \dot{V} &= e \left[ \dot{w}_{ref} - \frac{1}{j} \left[ \frac{3P}{2} \left( (L_d - L_q) i_d i_q + \lambda_m i_q \right) - B w_r - T_L \right] \right] \\ &= -k e^2 + e \left( k e + \dot{w}_{ref} - \frac{3P \lambda_m}{2j} i_q + B w_r + T_L \right) - \frac{3P}{2j} (L_d - L_q) i_d i_q e \end{aligned} \tag{24}$$

When the following stabilizing function is defined, speed control tracking will be successful.

$$i_{qref} = \frac{2j}{3P \lambda_m} (k e + \dot{w}_{ref} + B w_r + T_L) \tag{25}$$

$$i_{dref} = 0 \tag{26}$$

The value of the energy function is reduced to zero by obtaining the appropriate control signal that will take the error to zero. Accordingly,  $V \leq 0$  allows us to generate the control signal whose condition is suitable for  $V > 0$ . The derivative of the energy function, including system dynamics, is as in Equation (24). The  $i_d$  and  $i_q$  in Equation (24) are our control parameters. By choosing the appropriate  $i_{dref}$  and  $i_{qref}$ ,  $\lim_{t \rightarrow \infty} v(t) \rightarrow 0$  is obtained for the energy function.  $i_{dref} = 0$  can be used for PMSMs. In this case, the candidate  $i_{qref}$  function is written as in Equation (25).

If Equations (25) and (26) are put in Equation (24), Equation (27) is determined as follows:

$$\dot{V} = -k e^2 < 0 \tag{27}$$

Consequently, the control signal is asymptotically stable.

### Disabling Undefined Range of the Derivative

Due to the  $w_{ref}$  in the BLT speed controller unidentified situations come into question in application of step speed. In order to relieve the control signal from the unspecified first and second derivative of the reference speed over time, a second order system is applied to the step speed as shown in Figure 6.

There are studies in the literature in which ramp [61], sinusoidal reference speed [61,62], or fixed reference speed [63,64] are used, the first and second derivatives of the reference speed are considered limited and this undefined range is omitted [65], the derivative of the reference speed is considered zero [61], and smoothed reference speed [66] is used.

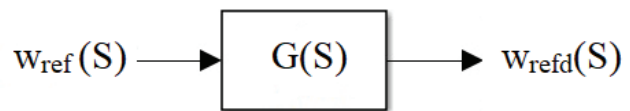


Figure 6. Block diagram of low-pass filter applied to the reference speed.

Here, for  $L\{\bullet\}$  Laplace transform operator, the transfer function of the low-pass pre-filter which is designed to be  $w_{ref}(s) = L\{w_{ref}(t)\}$  will be as follows:

$$G(s) = \frac{K \cdot w_n^2}{(s-s_1)^2} \tag{28}$$

If we excite Equation (28) with a step input ( $K = 1$ ),

$$Y(S) = \frac{w_n^2}{s(s^2 + 2\xi w_n s + w_n^2)} \tag{29}$$

The solution of Equation (29) in the time domain varies depending on the damping factor. For the critically damped case ( $\xi = 1$ ),

$$Y(S) = \frac{w_n^2}{s(s+w_n)^2} \tag{30}$$

Solution of Equation (30) in time domain,

$$y(t) = 1 - e^{-w_n \cdot t} (1 + w_n \cdot t) \tag{31}$$

Due to the exponential term in Equation (31), the range in which the derivative is undefined had been made ineffective.  $w_{refd}(s)$  is applied to the system which is obtained by selecting and 100 Hz for TF given in Equation (28), by considering the rise time of the system shown in Figure 8. In the pre-filter design, the selection of the frequency is determined by considering the rise time of the system so that the designed prefilter does not negatively affect the settling time of the system. This situation is shown in Figure 8. The response for the unit step input of the designed low-pass filter is shown in Figure 7.

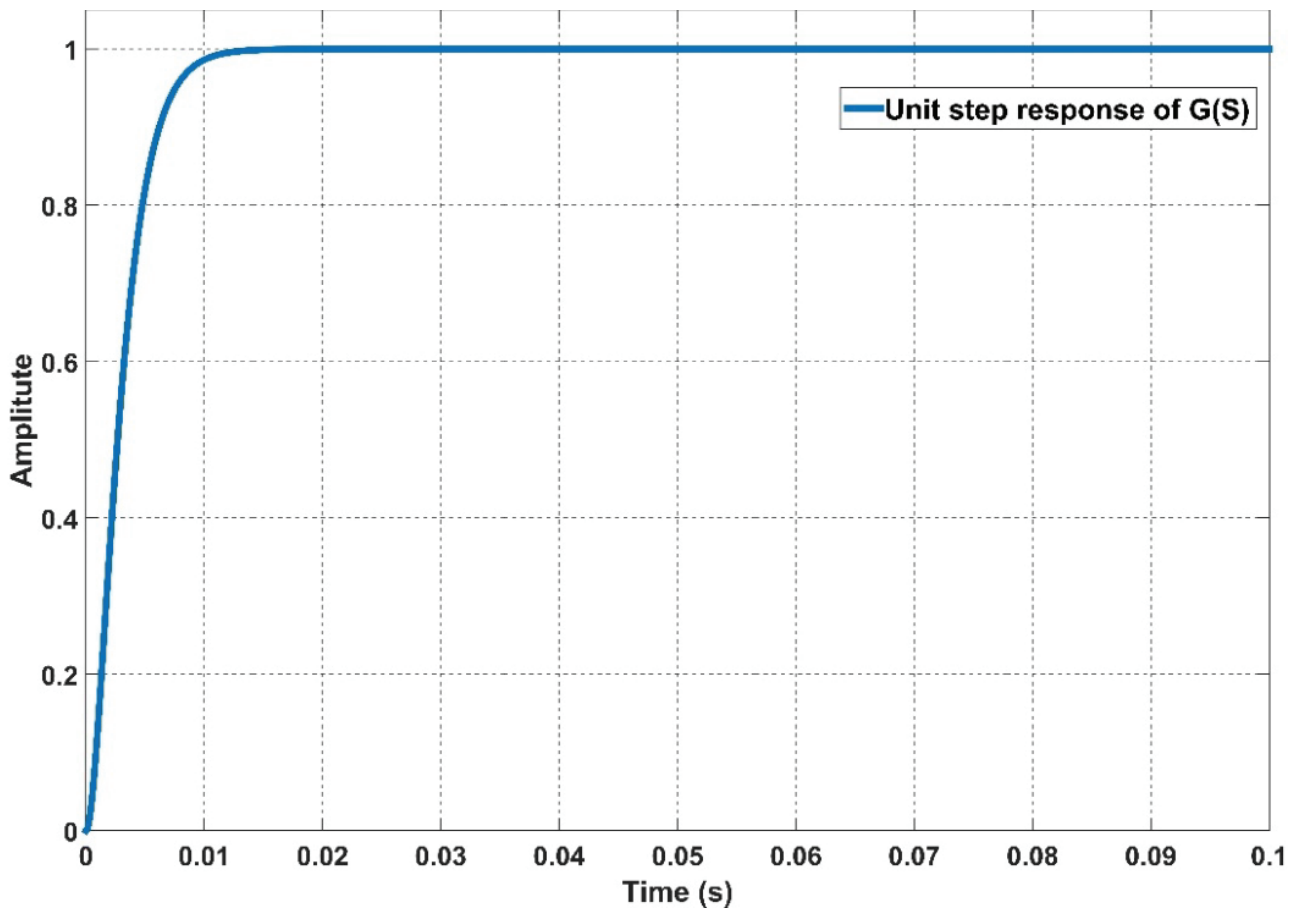


Figure 7. Unit step response of  $G(S)$ .

This way,  $w_{ref} \rightarrow \infty$  problem is solved by smoothing step speed change and the undefined state in the first derivative of the reference speed is eliminated. In order to compare the PI and BLT speed controllers under equal conditions, a smoothed speed is applied to both.

Table 2. PMSM Parameters

Parameters	Value	Unit
Moment of Inertia	0.00012	kg m <sup>2</sup>
Inductances ( $L_q=L_d$ )	16	mH
Stator Winding Resistance	5.2	$\Omega$
Rotor Magnetic Flux	0.345	Wb
Rated Power	1.1	kW
Pole Number	6	

### Simulation Studies

FOC simulation of PMSM is performed in MATLAB/Simulink with PI and BLT speed control techniques. Sampling time  $1 \mu\text{s}$  and switching frequency 10 kHz are the parameters shown in the Table 2 [25]. The figures of both methods are shown in Figures 8 to 16. The performance of

the methods in simulation studies is given in Tables from 3 to 14. Viscous friction is neglected in this study.

Three different simulation studies are conducted in order to compare PI and BLT speed controllers. These studies are; (1) reference speed is changed and reference torque is kept constant; (2) the reference speed is kept constant and the reference torque is changed; (3) the winding resistance is changed under constant reference speed and torque. The step function is used in all simulations and the duration is 1.5 sec. The smoothed reference signal obtained with the designed low-pass filter is used in step speed changes.

Simulation – 1 is named as “Variable Speed and Constant Torque Simulation” and is represented by S1. Simulation – 2 is named as “Constant Speed and Variable Torque Simulation” and is represented by S2. Simulation – 3 is named as “Constant Speed and Constant Torque Simulation” and is represented by S3. Three simulations are applied separately for both the designed PI speed controller and the proposed BLT speed controller. The number of analyzed simulations is 6. The steady-state response of S1 and S3 is analyzed. Both the transient response and the steady state response of S2 are analyzed. In this study, 8 different cases are created for simulations and these are explained with sub-headings.

The aim is to analyse the responses of the rotor speed that the speed controllers designed in each simulation will show under different conditions. These conditions are determined and applied as sudden changes in speed in S1, sudden changes in torque in S2, heating and partial short circuit conditions that may occur in stator windings in S3. Torque performance of the controllers in the first two simulations is also compared. Transient responses of PI and BLT speed controllers in S2 and S3 are investigated.

In this study, the RMSE performance criterion is selected to examine the steady-state response in cases where speed, torque or resistance changes occur. RMSE values are calculated separately according to the time intervals of the changes. The ITAE performance criterion is selected to calculate the errors that occur during the simulation. Thus, both the transient response and the steady state response of both controllers are examined.

Information on the purposes of these three different simulation studies, in which both speed controllers are used, is given in the “Case Descriptions” sub-heading.

## CASE DESCRIPTIONS

Cases of S1 are Case 1 and Case 2. Cases of S2 are Case 3, Case 4, Case 5 and Case 6. Cases of S3 are Case 7 and Case 8. In Case 1, Case 2, Case 3 and Case 4, the performances of the steady-state responses of the controllers are investigated. In Case 5, Case 6, Case 7 and Case 8, the performances of the transient responses of the controllers are examined.

Frequently used in the literature as performance criteria settling time, overshoot, peak value and time to reach this value, RMSE, ITAE criteria are selected.

### Case 1 and Case 2

Case 1 and Case 2 are the situation that the PI speed controller and the proposed BLT speed controller are used as the speed controller in S1, respectively. Steady state responses are investigated in Case 1 and Case 2.

In S1, while reference torque is 2.8 Nm, reference speed is applied in equal time periods (0.5 s) as 100, 200 and 150 rpm, respectively.

The purpose of S1 is to examine and compare the performance of the controllers in sudden changes in reference speed.

In S1, under constant load torque, the reference speed is changed in both directions with the step function.

The performance criteria of the speed and torque for both speed controllers are compared.

Case 1 and Case 2 are compared with the selected performance criteria. Table 3 and Table 4 are created with the results obtained. While the speed performances of the cases are given in Table 3, the torque performances of the cases are given in Table 4.

### Case 3 and Case 4

Case 3 and Case 4 are the situation that the PI speed controller and the proposed BLT speed controller are used as the speed controller in S2, respectively. Steady state responses are examined in Case 3 and Case 4.

In S2, while the reference speed is 100 rpm, the reference torque is applied as 2.8, 1.4 and 2.1 Nm in equal time periods (0.5 s), respectively.

The purpose of S2 is to examine and compare the robustness of the controllers against sudden changes in torque.

In S2, the reference load is changed in both directions with the step function to model the load torque disturbance.

The performance criteria of the speed and torque for both speed controllers are compared similar to the Case 1 and Case 2.

Case 3 and Case 4 are compared with the selected performance criteria and Table 5 and Table 6 are created with the results obtained. While the speed performances of the cases are given in Table 5, the torque performances of the cases are given in Table 6.

### Case 5 and Case 6

Case 5 and Case 6 are the situation that the PI speed controller and the proposed BLT speed controller are used as the speed controller in S2, respectively. Transient responses are investigated in Case 5 and Case 6.

The performance criteria of the speed for both speed controllers are compared. For this, response time (Res. T) and RMSE criteria are selected.

Case 5 and Case 6 are compared with the selected performance criteria and Table 7 is created with the results obtained.

In Table 7, transient response performances of the speed at the time of torque change are given.

### Case 7 and Case 8

Case 7 and Case 8 are the situation that the PI speed controller and the proposed BLT speed controller are used as the speed controller in S3, respectively. Transient responses are examined in Case 7 and Case 8.

While the temperature rise in the stator winding resistance increases the resistance, possible partial short circuits in the windings reduce the resistance. In the name of robustness analysis, both reference speed tracking against torque change and reference speed tracking against resistance changes have been obtained and compared. The comparison has also been made in the transient and its figures are included.

In S3, when reference speed is 100 rpm and reference torque is 2.8 Nm, stator winding resistance is changed from R to 1.2R and R to 0.8R, respectively.

The purpose of S3 is to examine and compare the robustness of the controllers against parameter uncertainty.

In S3, the resistance is changed in both directions with the step function to model parameter uncertainty.

The performance criteria of the speed for both speed controllers are compared. Hence, Res. T and RMSE criteria are selected.

Case 7 and Case 8 are compared with the selected performance criteria and Table 8 is prepared with the results obtained.

In Table 8, transient response performances of the speed at the time of winding resistance change are given.

**RESULTS AND DISCUSSION**

The figures comparing the reference speed and rotor speeds in the simulation studies of both techniques are as follows:

The tables with the comparisons which are applied for the performance criteria indicated in the simulation studies of both techniques are given below.

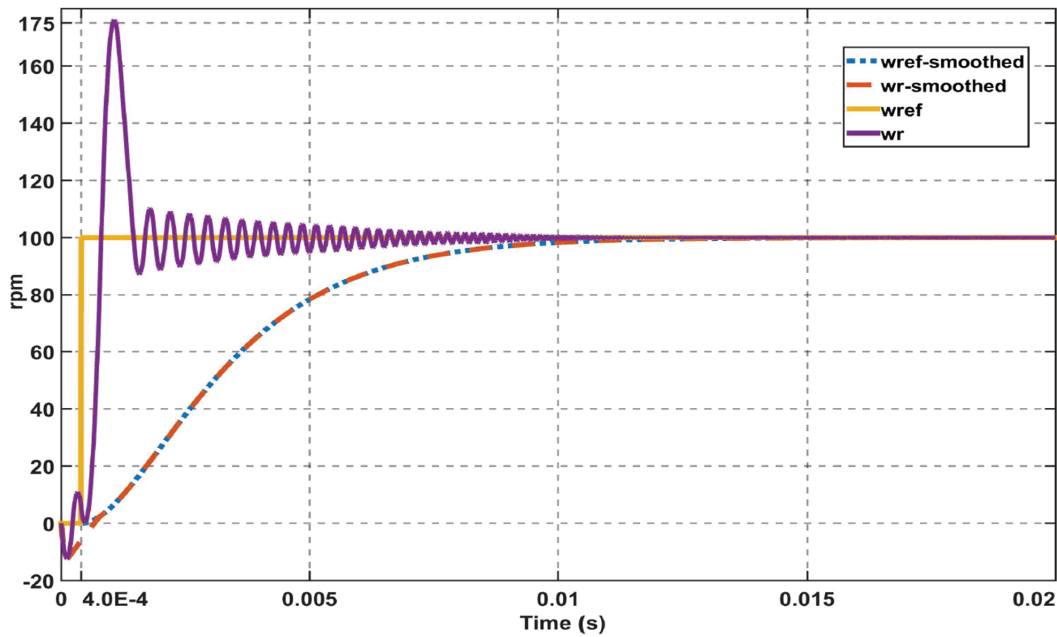


Figure 8. BLT speed controller speed with and without pre-filter.

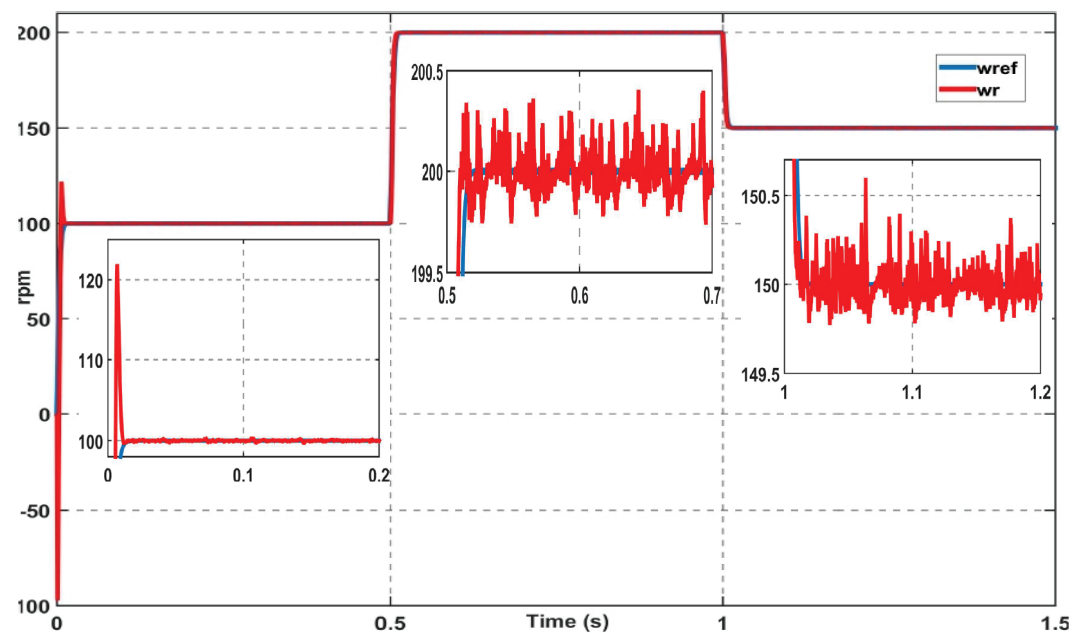


Figure 9. PI speed controller (Case 1) speed.

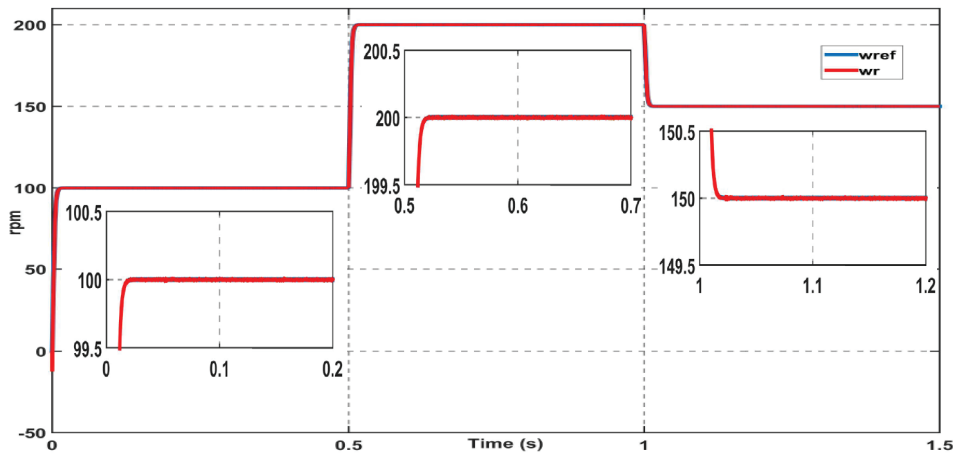


Figure 10. Figure 10. BLT speed controller (Case 2) speed.

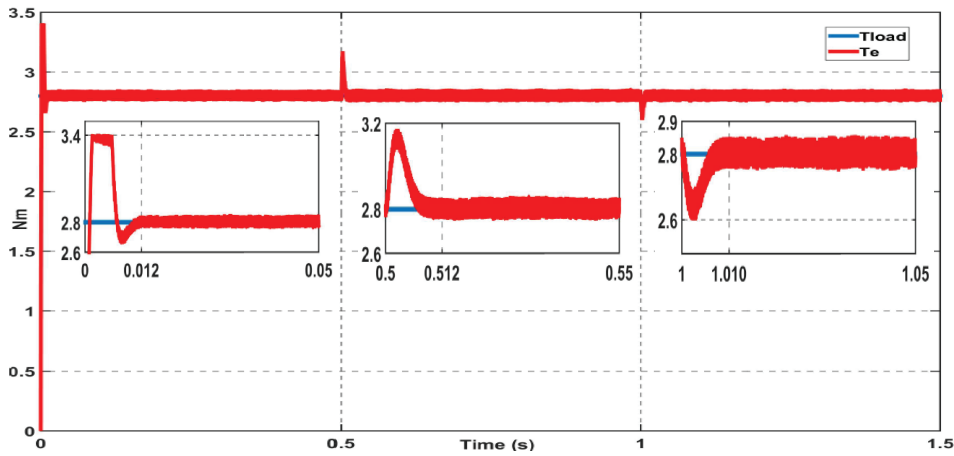


Figure 11. PI speed controller (Case 1) torque.

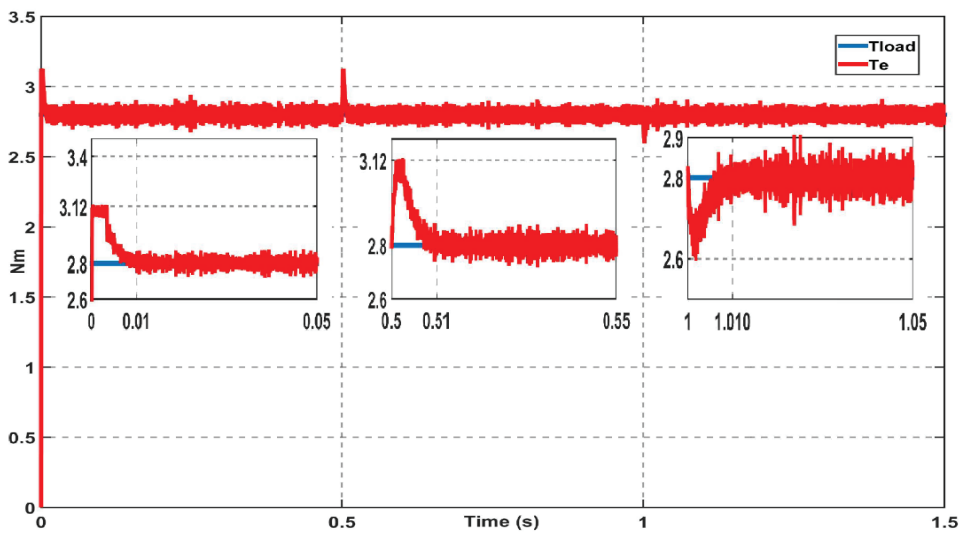


Figure 12. BLT speed controller (Case 2) torque.

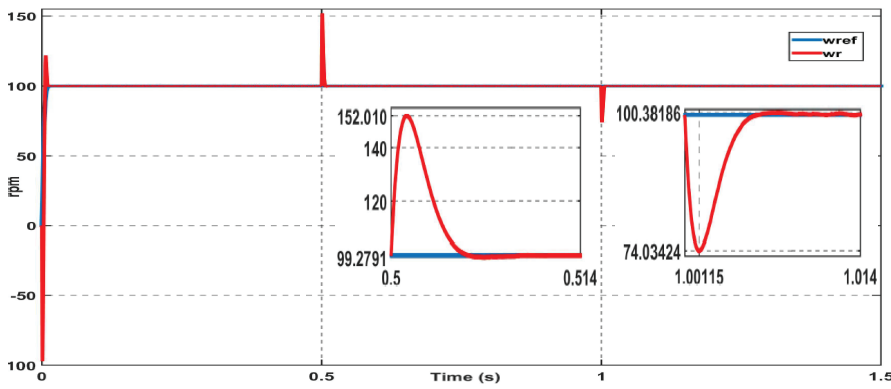


Figure 13. PI speed controller (Case 3 and Case 5) speed.

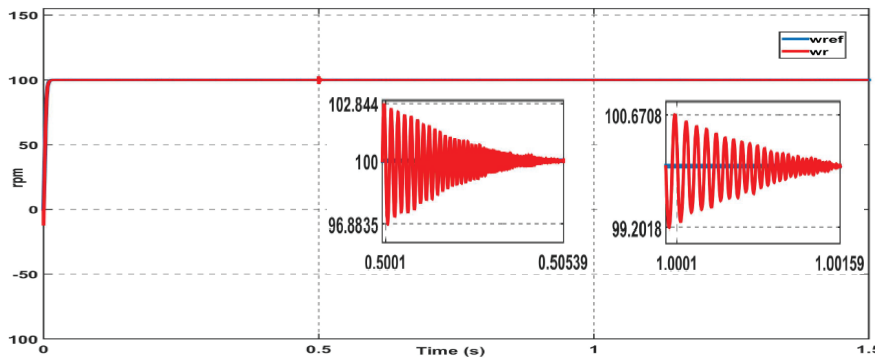


Figure 14. BLT speed controller (Case 4 and Case 6) speed.

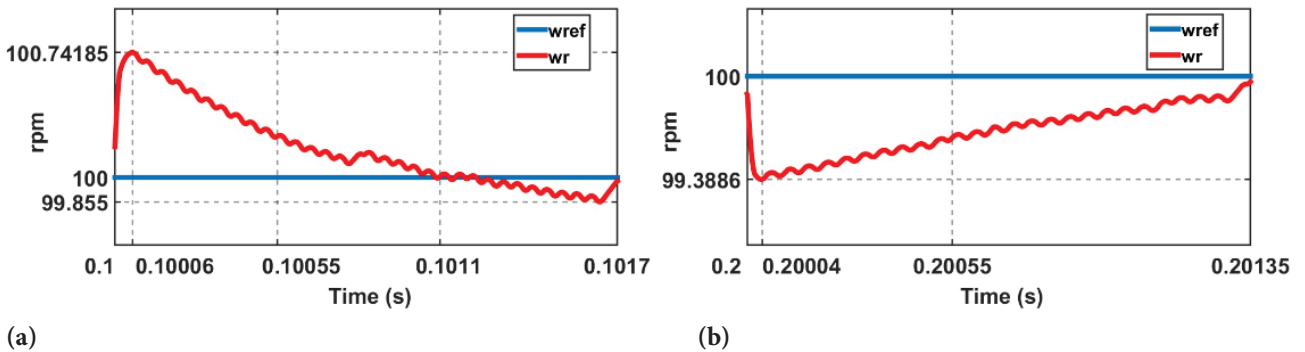


Figure 15. PI speed controller simulation 3 ETSR\_R (Case 7), (a) R-1.2R, (b) R-0.8R.

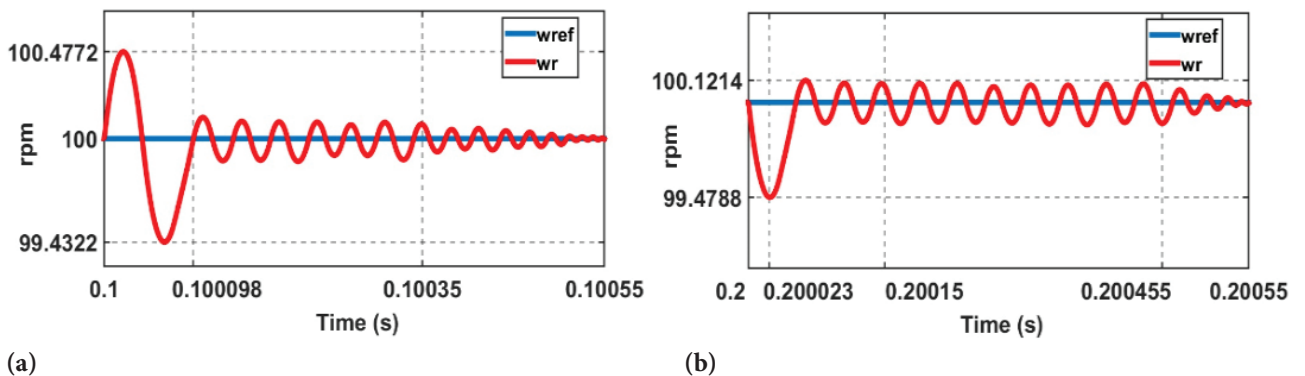


Figure 16. BLT speed controller simulation 3 ETSR\_R (Case 8), (a) R-1.2R, (b) R-0.8R.

**Table 3.** Performance criteria for S1: Speed Performances

PC	SSV_CT – Speed Performances					
	PI (Case 1)			BLT (Case 2)		
Ranges (s)	(0 – 0.5)	(0.5 – 1)	(1 – 1.5)	(0 – 0.5)	(0.5 – 1)	(1 – 1.5)
ST(ms)	14	15	15	--	--	--
OS.(%)	21.948	--	--	--	--	--
Peak	121.948	--	--	--	--	--
PT(ms)	6.8	--	--	--	--	--
RT(ms)	--	--	--	--	--	--
RMSE	0.0832	0.0964	0.0953	0.0017	0.0017	0.0017
ITAE	0.1246			0.0019		

**Table 4.** Performance criteria for S1: Torque Performances

PC	SSV_CT – Torque Performances					
	PI (Case 1)			BLT (Case 2)		
Ranges (s)	(0 – 0.5)	(0.5 – 1)	(1 – 1.5)	(0 – 0.5)	(0.5 – 1)	(1 – 1.5)
ST(ms)	12	12	10	10	10	10
OS.(%)	21.428	13.382	--	11.428	11.428	--
Peak	3.4	3.1747	--	3.12	3.12	--
PT(ms)	1.5-5.7	2.5	--	0.15-3.4	1-2.8	--
RT(ms)	--	--	--	--	--	--
RMSE	0.0187	0.0229	0.0212	0.0097	0.0093	0.0093
ITAE	0.0205			0.0067		

**Table 5.** Performance criteria for S2: Speed Performances

PC	SCV_ST – Speed Performances					
	PI (Case 3)			BLT (Case 4)		
Ranges (s)	(0 – 0.5)	(0.5 – 1)	(1 – 1.5)	(0 – 0.5)	(0.5 – 1)	(1 – 1.5)
ST(ms)	14	14	14	--	5.39	1.59
OS.(%)	21.948	52.01	--	--	2.844	0.6708
Peak	121.948	152.01	--	--	102.844	100.6708
PT(ms)	6.8	1.167	--	--	0.1	0.1
RT(ms)	--	--	--	--	--	--
RMSE	0.0832	0.1004	0.1017	0.0017	0.0017	0.0016
ITAE	0.2263			0.0037		

A large number of performance criteria are used to compare the performance of PI and BLT controllers.

If there is a reduction in the values indicated by these criteria for different controllers, this means that it is a performance improvement.

If there is a reduction in the value obtained for the performance criteria with the change of only the controller under the same conditions, this indicates that the used controller performs better.

**Table 6.** Performance criteria for S2: Torque Performances

PC	SCV_ST – Torque Performances					
	PI (Case 3)			BLT (Case 4)		
Ranges (s)	(0 – 0.5)	(0.5 – 1)	(1 – 1.5)	(0 – 0.5)	(0.5 – 1)	(1 – 1.5)
ST(ms)	12	7.3	7.3	10	5.39	1.59
OS.(%)	21.428	--	7.613	11.428	96.46	32.126
Peak	3.4	--	2.25988	3.12	2.7505	2.77465
PT(ms)	1.5-5.7	--	2 – 2.75	0.15-3.4	0.22	0.05
RT(ms)	0.7687	--	--	0.0902	--	--
RMSE	0.0187	0.0168	0.0181	0.0097	0.0097	0.0096
ITAE	0.0173			0.0070		

**Table 7.** Performance criteria for S2: ETSR\_T Performances

	Error of transient response of the speed at the time of torque change in S2			
	PI (Case 5)		BLT(Case 6)	
CS	2.8Nm→1.4Nm	1.4Nm→2.1Nm	2.8Nm→1.4Nm	1.4Nm→2.1Nm
C. Time	0.5	1.0	0.5	1.0
Res.T(ms)	14	14	5.39	1.59
RMSE	19.0685	9.5167	1.0494	0.2860

**Table 8.** Performance criteria for S3: ETSR\_R Performances

	Error of transient response of the speed at the time of winding resistance change in S3			
	PI (Case 7)		BLT (Case 8)	
CS	R→1.2R	R→0.8R	R→1.2R	R→0.8R
C. Time	0.1	0.2	0.1	0.2
Res.T(ms)	1.7	1.35	0.55	0.55
RMSE	0.3035	0.3627	0.1683	0.1328

**Table 9.** Performance Improvement According to Table 3

PC	S1 Speed Performance Improvement (%Reduction)		
	(0 – 0.5)s	(0.5 – 1)s	(1 – 1.5)s
ST	%100	%100	%100
OS	%100	--	--
Peak	%100	--	--
PT	%100	--	--
RMSE	%97.9567	%98.2365	%98.2162
ITAE	%98.4751		

The results obtained according to the performance criteria selected for all cases of all simulations are given in Table 3 to Table 8.

The improvement in controller performance is defined as the % reduction in performance criteria used in Tables 3 to 8.

Table 9 is created to see the improvement in speed performance when using BLT speed controller (Case 2) instead of PI speed controller (Case 1) in S1. For this, the data in Table 3 is analyzed.

Table 10 is prepared to see the improvement in torque performance as using BLT speed controller (Case 2) instead of PI speed controller (Case 1) in S1. For this, the data in Table 4 is analyzed.

Table 11 is created to see the improvement in speed performance when using BLT speed controller (Case 4) instead

of PI speed controller (Case 3) in S1. For this, the data in Table 5 is analyzed.

Table 12 is prepared to see the improvement in torque performance as using BLT speed controller (Case 4) instead of PI speed controller (Case 3) in S1. For this, the data in Table 6 is analyzed.

Table 13 is created to see the improvement in transient response performances of the speed at the time of torque change when using BLT speed controller (Case 6) instead of PI speed controller (Case 5) in S2. For this, the data in Table 7 is analyzed.

Table 14 is prepared to see the improvement in transient response performances of the speed at the time of winding resistance change as using BLT speed controller (Case 8) is used instead of PI speed controller (Case 7) in S3. For this, the data in Table 8 are analyzed.

**Table 10.** Performance Improvement According to Table 4

PC	S1 Torque Performance Improvement (%Reduction)			
	Ranges	(0 – 0.5)s	(0.5 – 1)s	(1 – 1.5)s
ST		%16.6667	%16.6667	%0
OS		%46.6679	%14.6017	--
Peak		%8.2353	%1.7230	--
PT		%50.6944	%24	--
RMSE		%48.1283	%59.3886	%56.1321
ITAE		%67.3171		

**Table 11.** Performance Improvement According to Table 5

PC	S2 Speed Performance Improvement (%Reduction)			
	Ranges	(0 – 0.5)s	(0.5 – 1)s	(1 – 1.5)s
Ranges		%100	%61.5	%88.6429
ST		%100	%94.5318	-%100
OS		%100	%94.5318	-%100
Peak		%100	%91.4310	-%100
PT		%97.9567	%98.3068	%98.4267
RMSE		%98.3650		

**Table 12.** Performance Improvement According to Table 6

PC	S2 Torque Performance Improvement (%Reduction)			
	Ranges	(0 – 0.5)s	(0.5 – 1)s	(1 – 1.5)s
ST		%16.6667	%26.1644	%78.2192
OS		%46.6679	-%100	-%321.9887
Peak		%8.2353	-%100	-%22.7786
PT		%50.6944	-%100	%97.8947
RMSE		%48.1283	%42.2619	%46.9613
ITAE		%59.5376		

**Table 13.** Performance Improvement According to Table 7

PC	S2 Transient Speed Response Performance Improvement (%Reduction)	
C. Time	0.5 s	1 s
Res.T(ms)	%61.5	%88.6429
RMSE	%94.4967	%96.9948

**Table 14.** Performance Improvement According to Table 8

P.C.	S3 Transient Speed Response Performance Improvement (%Reduction)	
C. Time	0.1 s	0.2 s
Res.T(ms)	%67.6471	%59.2593
RMSE	%44.5470	%63.3857

For any performance criterion, if a value is obtained for the criterion when a PI controller is used, but a value is not obtained for the criterion when a BLT controller is used, the reduction used in the meaning of maximum improvement for the performance criterion is shown as 100%. In the reverse case, -100% is used. In the absence of data for both controllers, no data is written. If there is no improvement when using the BLT speed controller, the reduction is given a negative value.

When Figure 9 of the Case 1 and Figure 10 of the Case 2 are investigated, it is seen that the BLT speed controller has better speed performance in transient response and in steady state response.

If Figure 11 of the Case 1 and Figure 12 of the Case 2 are examined, it is determined that the BLT speed controller has better torque performance in transient response and in steady state response.

When Figure 13 of the Case 3 and Case 5, and Figure 14 of the Case 4 and Case 6 are investigated, it is seen that the BLT speed controller has better speed performance in transient response (Case 5 and Case 6) and in steady state response (Case 3 and Case 4).

If Figure 15 of the Case 7 and Figure 16 of the Case 8 are examined, it is found out that the BLT speed controller has better speed performance, becomes steady state in a shorter time and reaches the reference speed more rapidly.

When Table 3 of the Case 1 and Case 2 are investigated, in which the speed performances of the controllers is compared, it is seen that the BLT speed controller followed the smoothed reference speed perfectly without any overshoot, and has much better RMSE and ITAE values.

If Table 4 of the Case 1 and Case 2 are examined, in which the torque performances of the controllers is compared, it is determined that the BLT speed controller has a better settling time value, although the settling time of the controllers are close to each other, and the BLT speed controller has better values in other performance criteria including RMSE and ITAE.

When Table 5 of the Case 3 and Case 4 are investigated, in which the speed performances of the controllers is compared, it is found out that the BLT speed controller followed the smoothed reference speed almost perfectly with little overshoot and settling time, and has better RMSE and ITAE values.

If Table 6 of the Case 3 and Case 4 are examined, in which the torque performances of the controllers is compared, it is seen that the BLT speed controller has better values in all performance criteria except the percent overshoot and peak values in the 2nd and 3rd time intervals.

When Table 7, which compares the speed performances of Case 5 and Case 6 in the transient regime, is investigated, it is seen that the BLT speed controller has a much shorter Res. T and RMSE value. In other words, it is determined that the BLT speed controller is a more robust controller against sudden changes in torque.

If Table 8, which compares the speed performances of Case 7 and Case 8 in the transient regime, is examined, it is found out that the BLT speed controller has a shorter Res. T and RMSE value. In other words, it is determined that the BLT speed controller is a more robust controller against sudden changes in winding resistance.

The performance improvement achieved by using the proposed BLT controller is shown in Tables 9 to 14. When the data in the tables are investigated in case of a change in speed, torque and winding resistance, it is seen that the proposed BLT speed controller outperforms the PI speed controller designed with pole assignment method. This outperformance is seen in all cases for the RMSE and ITAE values. There are some disadvantages of the proposed BLT controller. The first of these is the minor increase the values of the overshoot, peak and peak time of the speed that occurs when the torque changes from 1.4 Nm to 2.1 Nm, as shown at Table 11. The second of these is the increase the values of the overshoot and peak of the torque that occurs when the torque changes from 1.4 Nm to 2.1 Nm, as shown at Table 12. And the last one is the increase the values of the overshoot, peak and peak time of the torque that occurs

when the torque changes from 2.8 Nm to 1.4 Nm, as shown at Table 12. Since main focus of this study is the minimization of PMSM steady-state speed error, it is determined that these disadvantages do not prevent reaching this aim. There is no change in the value of the settling time of the torque that occurs when the speed changes from 200 rpm to 150 rpm, as shown at Table 10. In all other situations where data is available, it is found out that performance criteria are improved by using the proposed BLT controller.

The outcomes of the simulations show that the proposed BLT controller has better performance in transient response and steady state response than PI controller.

The PI controller has not performed more satisfactorily than the proposed BLT controller at the overshoot during the transient response.

The results of the S1 show that the speed and torque performances of the proposed BLT controller are better than the PI controller.

The outcomes of S1 and S2 show that the RMSE values of the speed performance of the proposed BLT controller are not affected by the speed and torque changes. In addition, it is determined that the RMSE values of torque performance are not affected by the changes.

In all cases, it is found out that the proposed BLT controller has a rapid transient response and reaches steady state in a shorter time. This shows the robustness of the proposed BLT controller in all simulations where speed, torque and winding resistance change respectively for the robustness test. In other words, the proposed BLT controller performs better against load torque disturbance and parameter uncertainty.

## CONCLUSION

In the study, BLT speed controller which produces a control signal using derivative of the reference speed, so as not to be affected by step changes of the reference speed is designed. It can be seen from the simulation results that the designed pre-filter provides two features. The first of these features is to prevent spike in the control signal during the step change of reference speed; The second is that it allows steady state errors to drop to zero.

In addition, it is seen from the results that the proposed BLT controller is a more robust controller compared to the PI controller designed with the pole assignment method, since it has an energy function that penalizes the speed error.

It is considered to carry out sensorless control studies with the controllers used as a future work.

## NOMENCLATURE

$V_d, V_q$	d-q axes voltages
$i_d, i_q$	d-q axes (frame of reference) currents
$\lambda_d, \lambda_q$	d-q axes (frame of reference) fluxes
$\lambda_m$	Permanent magnet flux
$L_d, L_q$	d-q axes (frame of reference) stator inductances

$w$	Electrical angular speed (inverter frequency)
$w_r$	Mechanical angular speed
$\theta$	Rotor position
$R$	Stator resistance
$P$	Number of pole pairs
$p$	Derivative operator
$T_e$	Electromagnetic torque
$T_L$	Load torque
$B$	Friction coefficient
$J$	Inertia of the motor
$\vec{V}$	SVPWM voltage vector
$v_\alpha, v_\beta$	Reference voltage vector components of $\alpha$ - $\beta$ frame
$i_\alpha, i_\beta$	Reference currents of $\alpha$ - $\beta$ frame
$V_a, V_b, V_c$	Inverter terminal voltages
$V_{dc}$	Inverter supply voltage
$\vec{V}_k$	k sector space vector
$\vec{V}_{k+1}$	k+1 sector space vector
$\vec{V}_{ref}$	Average space vector
$T_s$	Switching period
$T_k$	Half of the $\vec{V}_k$ run time
$T_{k+1}$	Half of the $\vec{V}_{k+1}$ run time
$T_0$	Half of the zero state time
$\omega$	Frequency of the desired phase voltage in SVPWM
$\vec{i}_s$	Stator complex current vector
$\vec{i}_a, \vec{i}_b, \vec{i}_c$	Stator phase current vectors
$\vec{i}_s$	Complex stator current vector
$\alpha, \alpha^2$	Spatial operators
$w_c$	Corner frequency
$k_p$	Proportion gain coefficient
$k_i$	Integral gain coefficient
$k_t$	Torque Constant
$\xi$	Damping ratio
$w_n$	Underdamped natural frequency
$w_0$	Natural frequency of second order system
$e$	Speed error (Trajectory tracking error)
$\dot{e}$	First derivative of speed error
$w_{ref}$	Reference speed
$\dot{w}_{ref}$	First derivative of reference speed
$V$	Lyapunov function
$\dot{V}$	First derivative of Lyapunov function
$k$	Positive closed loop feedback constant
$i_{d,ref}, i_{q,ref}$	$i_d, i_q$ reference currents
$K$	Smoothing system gain

## Abbreviations Used in Tables

S1	Simulation 1
S2	Simulation 2
S3	Simulation 3
PC	Performance Criteria
ST	Settling Time
OS	Overshoot (%)
PT	Peak time (ms)
RMSE	Root Mean Squared Error

ITAE	Integral of Time weighted Absolute Error
CS	Change of state
C.Time	Change Time
Res.T	Response Time
ETSR_T	Error of transient speed response at torque change
ETSR_R	Error of transient speed response at winding resistance change
SSV_CT	Smoothed Step Velocity Constant Torque
SCV_ST	Smoothed Constant Velocity Step Torque

## AUTHORSHIP CONTRIBUTIONS

Authors equally contributed to this work.

## DATA AVAILABILITY STATEMENT

The authors confirm that the data that supports the findings of this study are available within the article. Raw data that support the finding of this study are available from the corresponding author, upon reasonable request.

## CONFLICT OF INTEREST

The author declared no potential conflicts of interest with respect to the research, authorship, and/or publication of this article.

## ETHICS

There are no ethical issues with the publication of this manuscript.

## REFERENCES

- [1] Nirowski G, Plackner K, Piepenbreier B, Tolle H. New permanent field synchronous motor with integrated inverters. In: Proceeding of ICEM'90; 1990. p. 124–131.
- [2] Rashid M. Power electronics handbook. 3rd ed. USA: Elsevier Inc.; 2011.
- [3] Xiao X, Chen C, Zhang M. Dynamic permanent magnet flux estimation of permanent magnet synchronous machines. IEEE Trans on Applied Superconductivity 2010;20:1085–1088. [\[CrossRef\]](#)
- [4] Proca AB, Keyhani A, El-Antably A, Lu W, Dai M. Analytical model for permanent magnet motors with surface mounted magnets. IEEE Trans Energy Convers 2003;18:386–391. [\[CrossRef\]](#)
- [5] Mohamed YAI. A Hybrid-type variable-structure instantaneous torque control with a robust adaptive torque observer for a high-performance direct-drive PMSM. IEEE Trans Ind Electron 2007;54:2491–2499. [\[CrossRef\]](#)
- [6] Krishnan R. Selection criteria for servo motor drives. IEEE Trans on Ind Appl 1987;23:270–275. [\[CrossRef\]](#)
- [7] Choi HH, Kim EK, Yu DY, Jung JW, Kim TH. Precise PI speed control of permanent magnet synchronous motor with a simple learning feedforward compensation. Electr Eng 2017;99:133–139. [\[CrossRef\]](#)
- [8] Balda JC, Pillay P. Speed controller design for a vector-controlled permanent magnet synchronous motor drive with parameter variations. In: Conference record of the 1990 IEEE industry applications society annual meeting USA; 1990. p. 163–168.
- [9] Adam AA, Elnady A. Adaptive steering-based HDTC algorithm for PMSM. Asian J Control 2019;1–19. [\[CrossRef\]](#)
- [10] Singh KV, Bansal HO, Singh D. A comprehensive review on hybrid electric vehicles: architectures and components. J Mod Transport 2019;27:77–107. [\[CrossRef\]](#)
- [11] Xiao X, Chen C. Reduction of torque ripple due to demagnetization in PMSM using current compensation. IEEE Trans Appl Superconductivity 2010;20:1068–1071. [\[CrossRef\]](#)
- [12] Binns KJ, Jabbar MA. High-field self-starting permanent-magnet synchronous motor. IEE Proceedings B, Electric Power Appl 1981;128:157–160. [\[CrossRef\]](#)
- [13] Sünter S, Altun H. Control of a permanent magnet synchronous motor fed by a direct AC-AC converter. Electr Eng 2005;87:83–92. [\[CrossRef\]](#)
- [14] Guven S, Usta MA, Okumus HI. An improved sensorless DTC-SVM for three-level inverter-fed permanent magnet synchronous motor drive. Electr Eng 2018;100:2553–2567. [\[CrossRef\]](#)
- [15] Hernandez OS, Magdaleno JR, Caporal RM, Huerta EB. HIL simulation of the DTC for a three-level inverter fed a PMSM with neutral-point balancing control based on FPGA. Electr Eng 2018;100:1441–1454. [\[CrossRef\]](#)
- [16] Campos PJ, Coria LN, Trujillo L. Nonlinear speed sensorless control of a surface-mounted PMSM based on a Thau observer. Electr Eng 2018;100:177–193. [\[CrossRef\]](#)
- [17] Choi Y, Choi HH, Jung J. Feedback linearization direct torque control with reduced torque and flux ripple for IPMSM drives. IEEE Trans Power Electron 2016;31:3728–3737. [\[CrossRef\]](#)
- [18] Jezernik K, Korelic J, Horvat R. PMSM sliding mode FPGA-based control for torque ripple reduction. IEEE Trans Power Electron 2013;28:3549–3556. [\[CrossRef\]](#)
- [19] Aliskan I, Gulez K, Tuna G, Mumcu TV, Altun Y. Nonlinear speed controller supported by direct torque control algorithm and space vector modulation for induction motors in electrical vehicles. Elektronika Ir Elektrotehnika 2013;19:41–46. [\[CrossRef\]](#)
- [20] Mumcu TV, Aliskan I, Gulez K, Tuna G. Reducing moment and current fluctuations of induction motor system of electrical vehicles by using adaptive field oriented control. Elektronika Ir Elektrotehnika 2013;19:21–24. [\[CrossRef\]](#)

- [21] Hasse K. Zum dynamischen Verhalten der asynchronmaschine bei Betrieb mit variablem Standardfrequenz und Standardspannung. *ETZ-A*. 1968;89:77–81.
- [22] Blaschke F. Das Prinzip der feldorientierung, die Grundlage für die TRNSVEKTOR-regelung von asynchronmaschinen. *Siemens Zeitschrift* 1971;45:757–768.
- [23] Utkin V, Guldner J, Shi J. Sliding mode control in electro-mechanical systems. 2nd ed. New York: CRC Press; 2009.
- [24] Bida VM, Samokhvalov DV, Al-Mahturi FS. PMSM vector control techniques - a survey. In: 2018 IEEE Conference of Russian young researchers in electrical and electronic engineering (ElConRus); 2018. p. 577–581. [\[CrossRef\]](#)
- [25] Acikgoz AI, Aliskan I. Comparison of inverter control techniques in field oriented control of permanent magnet synchronous motor. In: Turkish national committee of automatic control Turkey; 2016. p. 322–327.
- [26] Li Q, Huang S. A novel method to suppress mid-frequency vibrations with a high speed-loop gain for PMSM control. *J Power Electron* 2016;16:1076–1086. [\[CrossRef\]](#)
- [27] Åström KJ, Hagglund T. *Advanced PID Controller*. ISA instrumentation, systems and automation Society; 2006.
- [28] Lina W, Kun X, Lillo L, Empringham L, Wheeler P. PI controller relay auto-tuning using delay and phase margin in PMSM drives. *Chin J Aeronautics* 2014;27:1527–1537. [\[CrossRef\]](#)
- [29] Rao VMV. Performance analysis of speed control of dc motor using P, PI, PD and PID controllers. *Int J Eng Res Technol* 2013;2:60–66.
- [30] Ogata K. *Modern Control Engineering*. 5th ed. Prentice Hall Inc.; 2010.
- [31] Ziegler JG, Nichols NB. Optimum setting for automatic controllers. *Trans Am Soc Mech Eng* 1942;64:759–768. [\[CrossRef\]](#)
- [32] Shahat A, Shewy H. Permanent magnet synchronous drive system for mechatronics applications. *Int J Res Rev Appl Sci* 2010;4:323–328.
- [33] Zheng W, Luo Y, Pi Y, Chen Y. Improved frequency domain design method for the fractional order proportional-integral-derivative controller optimal design: a case study of permanent magnet synchronous motor speed control. *IET Control Theory Appl* 2018;12:2478–2487. [\[CrossRef\]](#)
- [34] Zheng W, Luo Y, Chen Y, Pi Y, Yu W. An improved frequency-domain method for the fractional order PI $\lambda$ D $\mu$  controller optimal design. In: 3rd IFAC conference on advances in proportional-integral-derivative control Belgium; 2018. p. 681–686. [\[CrossRef\]](#)
- [35] Zhang G, Furusho J. Speed control of two-inertia system by PI/PID control. *IEEE Trans Ind Electron* 2000;47:603–609. [\[CrossRef\]](#)
- [36] Cao X, Fan L. Real-time PI controller based on pole assignment theory for permanent magnet synchronous motor. In: Proceedings of the IEEE international conference on automation and logistics China; 2008. p. 221–215.
- [37] Suh G, Hyun DS, Park JI, Lee KD, Lee SG. Design of a pole placement controller for reducing oscillation and settling time in a two-inertia motor system. In: IECON'01 The 27th annual conference of the IEEE industrial electronics society; 2001. p. 615–620.
- [38] Chakraborty AK, Sharma N. Control of permanent magnet synchronous motor (PMSM) using vector control approach. In: 2016 IEEE/PES Transmission and distribution conference and exposition (T&D); 2016. p. 1–5. [\[CrossRef\]](#)
- [39] Wang L, Chai S, Yoo D, Gan L, Ng K. *PID and Predictive Control of Electrical Drives and Power Converters Using Matlab/Simulink*. New York: IEEE Press Wiley; 2015. [\[CrossRef\]](#)
- [40] Pilla R, Santukumari K. Design and simulation of the control system for inverter-fed permanent magnet synchronous motor drive. *Indonesian J Electr Eng Comput Sci* 2018;12:958–967. [\[CrossRef\]](#)
- [41] Lyapunov MA. Problème général de la stabilité du mouvement. *Ann Fac Sci Toulouse* 1907;9:203–474 (Translation of the original paper published in 1892 in *Comm Soc Math Kharkow* and reprinted as vol. 17 in *Ann. Math Studies*, Princeton University Press, Princeton, N.J., 1949). [\[CrossRef\]](#)
- [42] Quassaid M, Cherkaoui M, Nejmi A, Maaroufi M. Nonlinear torque control for PMSM: A Lyapunov technique approach. *World Acad Sci Eng Technol Int J Electr Comput Eng* 2007;1:918–921.
- [43] Shahgholian G, Hamidpour HR. Analysis and design of a nonlinear torque controller for PMSM drive system - A Lyapunov technique approach. *IJTPE J* 2014;6:70–76.
- [44] Quassaid M, Cherkaoui M, Zidani Y. A nonlinear speed control for a PM synchronous motor using an adaptive backstepping control approach. In: *IEEE ICIT* 2004;1287–1292.
- [45] Zaltni D, Sbita L, Abdelkrim MN. Nonlinear speed control using adaptive sliding mode and Lyapunov approaches for PMSM fed by a 3-levels NPC inverter. *J Electr Syst* 2010;6:350–360.
- [46] Prior G, Krstic M. Quantized-input control Lyapunov approach for permanent magnet synchronous motor drives. *IEEE Trans Control Syst Technol*. 2013;21:1784–1794. [\[CrossRef\]](#)
- [47] Khalil HK. *Nonlinear Systems*. 2nd ed. Prentice Hall Inc.; 1996.
- [48] Yıldız F, Aliskan I, Engin SN. Control of O<sub>2</sub> consumption in jet loop bioreactors by means of Lyapunov based nonlinear controller. In: *ELECO'08 Electrical-Electronics-Computer Symposium*. Turkey; 2016.

- [49] Implementing Space Vector Modulation with the ADMCF32X. Analog Devices Inc.; 2010;1–22.
- [50] Ramana P, Kumar BS, Mary KA, Kalavathi MS. Comparison of various PWM techniques for field oriented control VSI FED PMSM drive. IJAREEIE 2013;2: 2928–2936.
- [51] Space Vector Generator With Quadrature Control. Texas Instruments; 2012;1–12.
- [52] Kumar KV, Michael PA, John JP, Kumar SS. Simulation and comparison of SPWM and SVPWM control for three Phase Inverter. ARPN J Eng Appl Sci 2010;5:61–74.
- [53] Field Orientated Control of 3-Phase AC-Motors. Texas Instruments Europe; 1998;1–24.
- [54] Digital Motor Control Application Note SPRU485A. Texas Instruments; 2003.
- [55] Ogata K. System Dynamics. 4th ed. USA: Pearson Education Inc.; 2004.
- [56] Parks PC. A. M. Lyapunov's stability theory - 100 years on. IMA J Math Control Inf 1992;9:275–303. [\[CrossRef\]](#)
- [57] Slotine J, Li W. Applied Nonlinear Control. 4th ed. USA: Prentice Hall Inc.; 1991.
- [58] Fontes FACC, Magni L. A generalization of barbalat's lemma with applications to robust model predictive control. In: MTNS' 04 Proceedings of 16th International Symposium on Mathematical Theory of Networks and Systems. Belgium; 2004:1–5.
- [59] Lin CK, Liu TH, Fu LC. Adaptive backstepping PI sliding-mode control for interior permanent magnet synchronous motor drive systems. In: American Control Conference. 2011:4075–4080.
- [60] Wu Z, Xia Y, Xie X. Stochastic barbalat's lemma and its applications. IEEE Trans Automat Contr 2012;57:1537–1543. [\[CrossRef\]](#)
- [61] Khadija K, Benyounes M, Khalil BI, Rachid BM. A simple and robust speed tracking control of PMSM. Przegląd Elektrotechniczny (Electr Rev) 2011;87:202–207.
- [62] Karabacak M, Eskikurt HI. Speed and current regulation of a permanent magnet synchronous motor via nonlinear and adaptive backstepping control. Math Comput Model 2011;53:2015–2030. [\[CrossRef\]](#)
- [63] Kim W, Shin D, Chung CC. The Lyapunov-based controller with a passive nonlinear observer to improve position tracking performance of microstepping in permanent magnet stepper motors. Automatica 2012;48:3064–3074. [\[CrossRef\]](#)
- [64] Jon R, Wang Z, Luo C, Jong M. Adaptive robust speed control based on recurrent elman neural network for sensorless PMSM servo drives. Neurocomputing 2017;227:131–141. [\[CrossRef\]](#)
- [65] Yang Q, Zhu M, Jiang T, Fu K. Speed tracking control of permanent magnet synchronous motor based on high gain controller. In: ICMCA 2017 2nd International Conference on Mechanical Control and Automation 2017:46–51. [\[CrossRef\]](#)
- [66] Labiod S, Zibra A, Boubakir A. Backstepping speed control for permanent magnet synchronous motors with unknown load torque. In: ICEEA' 10th International Conference on Electrical Engineering, Electronics and Automatic 2010:1–5.